Separation Science and Technology
Publication details, including instructions for authors and subscription information:
http://www.informaworld.com/smpp/title~content=t713708471

Separation of Dilute CO_2-CH_4 Mixtures by Adsorption on Activated Carbon

F. Foeth[a]; M. Andersson[b]; H. Bosch[c]; G. Aly[b]; T. Reith[c]
[a] DEPARTMENT OF CHEMICAL TECHNOLOGY, UNIVERSITY OF TWENTE, NETHERLANDS [b] DEPARTMENT OF CHEMICAL ENGINEERING 1, UNIVERSITY OF LUND, LUND, SWEDEN [c] DEPARTMENT OF CHEMICAL TECHNOLOGY, UNIVERSITY OF TWENTE, AE ENSCHEDE, NETHERLANDS

To cite this Article Foeth, F. , Andersson, M. , Bosch, H. , Aly, G. and Reith, T.(1994) 'Separation of Dilute CO_2-CH_4 Mixtures by Adsorption on Activated Carbon', Separation Science and Technology, 29: 1, 93 — 118
To link to this Article: DOI: 10.1080/01496399408002471
URL: http://dx.doi.org/10.1080/01496399408002471

SEPARATION SCIENCE AND TECHNOLOGY, **29**(1), pp. 93–118, 1994

Separation of Dilute CO_2–CH_4 Mixtures by Adsorption on Activated Carbon

F. FOETH
DEPARTMENT OF CHEMICAL TECHNOLOGY
UNIVERSITY OF TWENTE
P.O. BOX 217, NL-7500 AE ENSCHEDE, NETHERLANDS

M. ANDERSSON
DEPARTMENT OF CHEMICAL ENGINEERING 1
UNIVERSITY OF LUND
P.O. BOX 124, S-221 00 LUND, SWEDEN

H. BOSCH
DEPARTMENT OF CHEMICAL TECHNOLOGY
UNIVERSITY OF TWENTE
P.O. BOX 217, NL-7500 AE ENSCHEDE, NETHERLANDS

G. ALY
DEPARTMENT OF CHEMICAL ENGINEERING 1
UNIVERSITY OF LUND
P.O. BOX 124, S-221 00 LUND, SWEDEN

T. REITH
DEPARTMENT OF CHEMICAL TECHNOLOGY
UNIVERSITY OF TWENTE
P.O. BOX 217, NL-7500 AE ENSCHEDE, NETHERLANDS

ABSTRACT

The adsorption separation process of diluted gas mixtures containing carbon dioxide and methane on activated carbon has been investigated. Experimental breakthrough curves for both the adsorption and desorption processes have been obtained using mixtures of one or two adsorbable components and one nonadsorbable. A parametric study was conducted to determine the influence of temperature, inlet partial pressure, and superficial velocity on the performance of the adsorption process. The separation factor for the activated carbon was determined to be

3–3.5 at 40°C and 2.7–2.8 at 60°C. The experimental curves have been calculated using a mathematical model based on the approximations of local equilibrium and isothermal conditions. The system of differential equations was solved numerically using a Crank–Nicolson finite difference discretization scheme. The resulting nonlinear system of equations was solved iteratively using the Gauss–Seidel method. The parameters in the model have been estimated either by empirical correlations or using experimental data. The model simulations for both the adsorption and desorption processes are generally in good agreement with experimental data. The evident deviations that resulted in a few cases can be attributed to deficiencies in the Langmuir model itself.

INTRODUCTION

Though used as a purification process over a long time period, it is only over the last two decades that adsorption has become well established in the chemical and hydrocarbon process industries for the bulk separation of components in a mixture. A broad range of zeolitic, carbonaceous, and polymeric adsorbents can be manufactured and tailored for specific separations. Useful and comprehensive reviews have recently been published covering almost all aspects of adsorption technology (1, 2).

This paper reports the experimental and simulation study of separation of dilute mixtures of CH_4 and CO_2 by adsorption on activated carbon. Methane–carbon dioxide separation is required in two important applications: landfill gas, which contains about 50% CO_2 as an impurity, and tertiary oil recovery, where the effluent gas contains up to 20–80% CO_2 and CH_4 (3).

Landfill gases contain mainly 50–65% CH_4 and 35–50% CO_2 as well as traces of N_2 from entrained air. They are generally available in the 230–370 kPa pressure range. For environmental and energy conservation reasons, it is important to recover methane as pipeline quality by enriching these gases to over 90%. Methane-rich landfill gases have recently been utilized as an alternative energy source by direct combustion in heating boilers and gas engines for production of thermal energy and electric power, respectively. Another method for utilization of landfill gases is upgrading and recovery of methane as synthetic natural gas by separation from CO_2. Different separation methods, such as physical and chemical absorption of CO_2, membrane permeation, and selective adsorption of CO_2, can be applied to achieve this goal.

Purification with activated carbons and subsequent gas separation with carbon molecular sieve-based pressure swing adsorption (PSA) is an attractive process to make available clean synthetic natural gas from landfill gases. Two full-scale plants for methane recovery from landfill gases are

now in operation in the Netherlands with a total capacity of 2200 m^3/h (4). Kinetic separation of CH_4–CO_2 mixtures by adsorption on carbon molecular sieves has recently been studied (3). Bulk gas separation and purification of CH_4–CO_2 mixtures by PSA on 4A/13X molecular sieves was also investigated using a simulated biogas mixture (5). Equilibrium constants, intracrystalline diffusivities, and heats of adsorption for O_2, N_2, CH_4, and CO_2 were measured in a chromatographic study of sorption and diffusion in 4A and 5A zeolites (6). It was concluded that dispersion of the chromatographic response for these components is controlled mainly by axial dispersion with some contribution from macropore diffusion.

To determine the performance of a fixed-bed adsorber, equilibrium data and breakthrough curves are necessary. The shape or the width of the breakthrough curve is crucially important in the design of adsorbers and other cyclic separation processes. In order to avoid excessive laboratory and pilot-plant facilities to obtain such data, adsorption models are used to simulate component breakthrough curves based on the available equilibrium, mass, and heat transfer data.

Modeling of multicomponent adsorption systems is scarcely reported in the literature. This is probably due to the lack of experimental multicomponent adsorption equilibrium data and breakthrough curves needed to verify model predictions. Different methods for calculating the breakthrough curves of binary systems have recently been reported. Basic equations were solved numerically by assuming pore diffusion kinetics for intraparticle diffusion (7). The linear driving force approximation, the validity of which is recognized for single-component systems, was also introduced (8, 9). Simpler solutions were obtained by imposing the constant pattern approximation (10, 11). It was also demonstrated (12) that an analytical solution can be obtained for a special case in which the adsorption isotherm is expressed by the Langmuir equation and the ratio of the overall mass transfer coefficients of the two components is unity. A simplified method was presented (13) for calculating the breakthrough time and the length of the mass transfer zone, where it was shown experimentally that a constant pattern holds in relatively long columns. Sircar and Kumar (14) studied the column dynamics for adsorption of bulk binary mixtures of N_2, CH_4, and CO_2 in the presence of nonadsorbing He and for adsorption of CO_2–CH_4 and CO_2–N_2 on activated carbon. They concluded that the dynamic behavior of these adsorption systems can be described very well by using the adiabatic, isobaric, constant pattern model for column adsorption and linear driving force models for mass transfer. Empirical correlations for calculating mass transfer coefficients may only provide an order of magnitude calculation of the mechanisms of adsorption.

The various mathematical models commonly used to describe an adsorption column differ in their generality depending on the extent of the approximations introduced (15–23). However, all models have two assumptions in common: there is no pressure drop over the bed and there are no radial concentration or temperature gradients. In all models except that of Wong and Niedzwiecki (16), thermal equilibrium is assumed.

The main objective of this work was to investigate the influence of different operating parameters on the breakthrough behavior of methane and carbon dioxide. Another objective was to determine the adsorption isotherms for each species at different temperatures. The experiments were thus conducted in a chromatographic mode by using He as a carrier gas. The experimental results were used to test the applicability of the equilibrium-dispersed plug flow model in describing the adsorption and desorption of dilute mixtures of CH_4 and CO_2.

EXPERIMENTAL

Experimental Setup

The experimental setup was designed to measure breakthrough curves for two different systems: binary gas mixtures with one adsorbable component and one inert carrier gas, CO_2 + He or CH_4 + He, and ternary mixtures with two adsorbable components and one inert carrier gas, CO_2 + CH_4 + He. The measurements could be performed at various temperatures and flow rates at pressures between 1 and 2.5 bar. The experimental setup is shown schematically in Fig. 1. The adsorption column was installed in a gas chromatograph (GC) manufactured by Varian (type 3400). The column was filled with a commercial activated carbon. The characteristics of the adsorber column are summarized in Table 1.

The GC was equipped with a thermal conductivity detector (TCD) and a flame ionization detector (FID), and it had been rebuilt to measure breakthrough curves. The gas mixture with the adsorbable components could

TABLE 1
Characteristics of the Adsorption Column

Weight of the adsorbent	0.0164 kg
Length of the fixed bed	0.147 m
Internal diameter of the column	0.0168 m
Mean equivalent diameter of the particles	0.00148 m
External void fraction	0.38
Porosity (internal void fraction)	0.357
Solid bulk density	503 kg/m^3

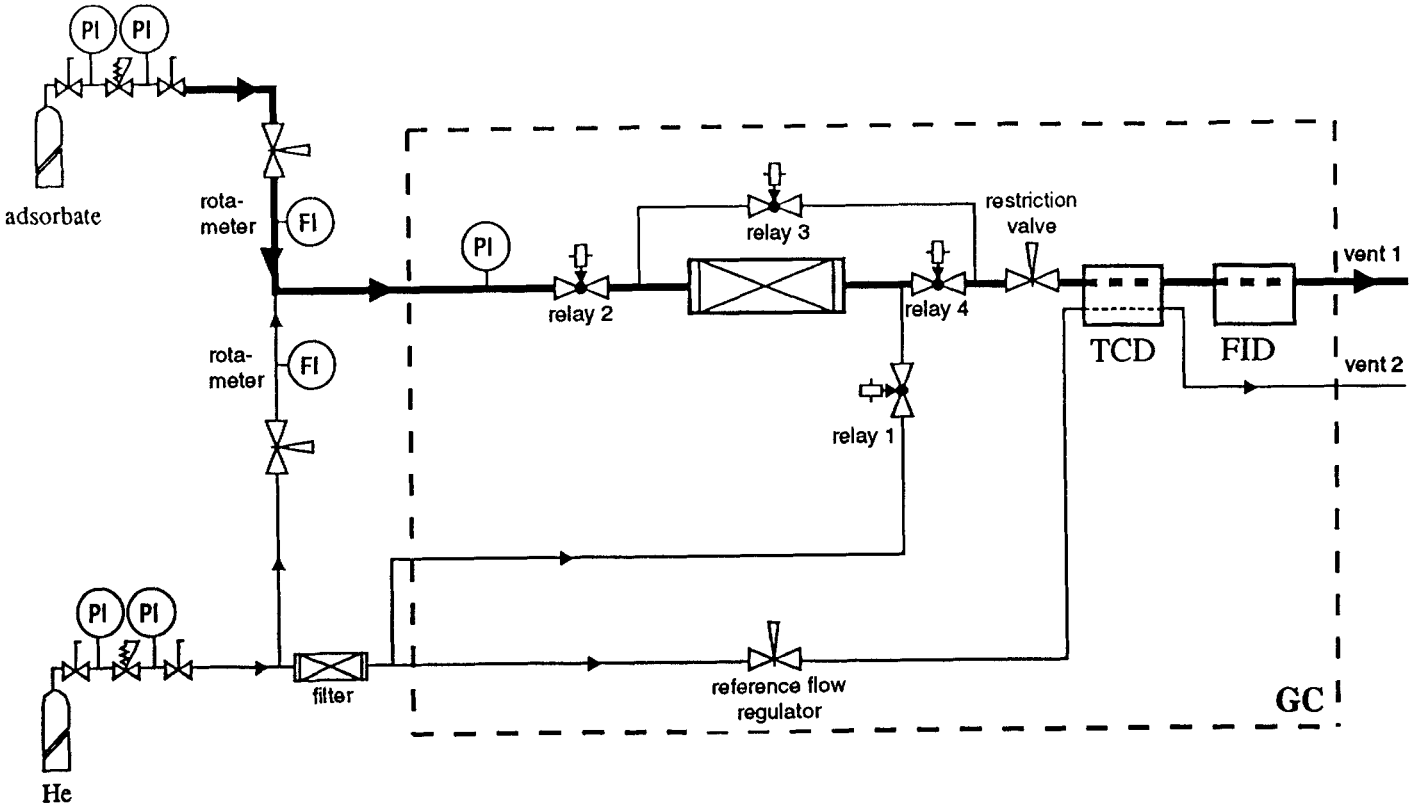

FIG. 1 Schematic flow sheet of the experimental setup.

therefore be fed continuously to the column. This setup made it possible to measure the concentration of the adsorbates continuously at the outlet of the column during the experiment. For the binary mixture experiments, only the TCD was used to measure the concentration of the adsorbates. For the ternary mixture experiments, the FID signal determined the concentration of CH_4 while the concentration of CO_2 was determined from the weighted difference between the FID and TCD signals. Figures 2 and 3 show calibration data for the FID and TCD detectors for the single and binary adsorbable components in the carrier gas, respectively. In these figures the detector signals are plotted as functions of the mole fraction of the adsorbable component. It was also possible to purge the column in a countercurrent direction and to by-pass the column. This was controlled by four automatically controlled two-way solenoid valves, denoted as relays 1–4 in Fig. 1.

The flow rates from the adsorbate gas bottle and the carrier gas bottle were controlled by two rotameters. The concentration of the gas entering the column was controlled by adjusting the flow rates of the two gas streams. The pressure was measured by a pressure transducer while the temperature of the oven was controlled automatically by the GC. The

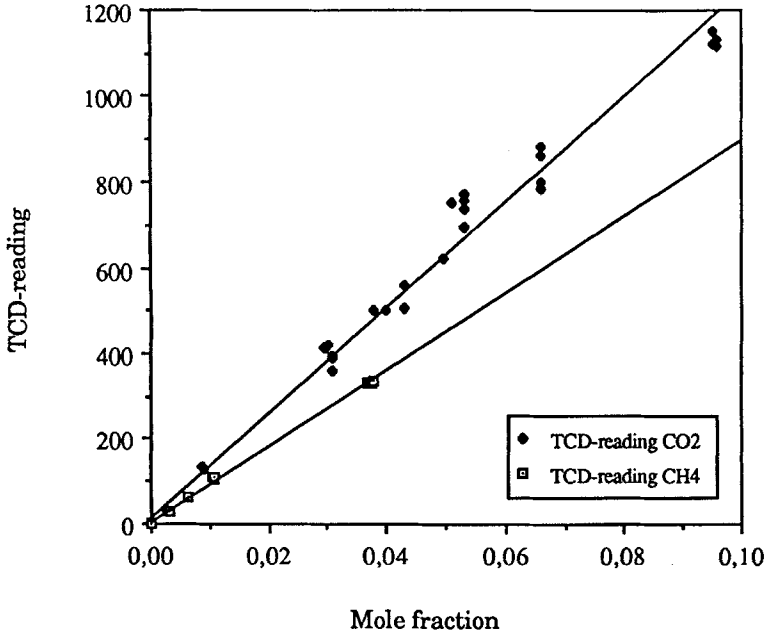

FIG. 2 Calibration curves for the thermal conductivity detector (TCD).

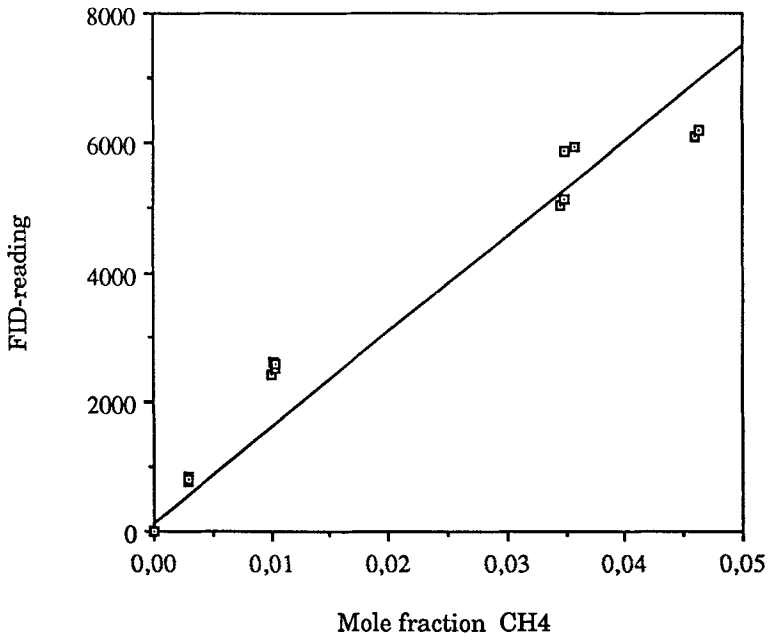

FIG. 3 Calibration curve for the flame ionization detector (FID).

flow rate was measured after the chromatograph with a digital bubble flowmeter (manufactured by Varian, type Optiflow 520) at the exit of the system.

Chemicals

The adsorbent was extrudate of activated carbon, cylindrical particles 1.0 mm in diameter and 2.16 mm long, manufactured by Norit (type RB1). Table 2 displays relevant data concerning the porous structure of the adsorbent used in this study. The carrier gas used in all experiments was helium, 99.995% pure and supplied by Hoekloos. Different gas mixtures were prepared using pure gas stocks. Carbon dioxide (99.998% pure) and methane (99.995% pure) were supplied by UCAR. The binary gas mixtures (9.5% CO_2 + 90.5% He and 11.8% CH_4 + 88.2% He) and the ternary gas mixture (12.0% CO_2 + 11.4% CH_4 + 76.6% He) were prepared by the high pressure laboratory at the University of Twente.

Experimental Procedure

The column was "conditioned" in order to remove any water or air adsorbed in the activated carbon. This was done for 14–15 hours by heat-

TABLE 2
Porous Structure Data of the Activated Carbon

P/P_0	Benzene adsorption (wt%)
0.9	36.8
0.7	35.9
0.5	35.4
0.3	34.9
0.1	31.8
0.07	31.2
0.03	29.8
0.01	27.5
0.005	24.6
0.001	19.8
Total pore volume	0.728 cm^3/g

ing the column to 200°C while it was purged with pure carrier gas. The column was conditioned after every change of the gas system. There was always a flow of carrier gas through the column after the conditioning to prevent any air from leaking into the system.

Each run started with an adjustment of the flow rate of the carrier gas through the column. The conditions in the column and the detector signal of the TCD and the FID were then allowed to stabilize before the breakthrough curve measurement started.

After each adsorption run, the column was desorbed with pure carrier gas. This operation was also recorded for most of the runs. Finally, the column was regenerated before the next run by increasing the column temperature to 145°C for 1 hour while still purging the column. After this, the column was swiftly cooled down and then allowed to stabilize for 1 hour. The baseline of the detector was used as a reference to make sure that the column was completely desorbed.

Design of Experiments

Data obtained from binary mixture experiments were used to calculate the adsorption isotherms for both carbon dioxide and methane. The experiments were also designated to investigate the effects of the operating parameters and the competitive adsorption of CO_2 and CH_4 on the breakthrough behavior. The measurements were performed at two different temperatures, 40 and 60°C, which are close to the temperatures at which PSA processes are often operated. The influence of the superficial velocity

was also investigated. The interval studied was 1.6 to 4.5 mm/s. Most experiments were performed twice in order to check the reproducibility.

Parameter Estimation

All experimental runs were compared with the mathematical model described below. The parameter values used in these simulations were estimated by using either semiempirical correlations from literature or experimental data. The Langmuir adsorption coefficients, b_i and $q_{i\infty}$, were determined from binary mixture experiments. The resulted values were used in the extended Langmuir equation describing the ternary system ($He/CO_2/CH_4$). The axial dispersion coefficient D_L was estimated from the empirical correlation valid for gases in packed beds (24):

$$D_L = 0.73\, D_M + \frac{ud_P}{2\left(1 + \dfrac{9.7D_M}{ud_P}\right)} \tag{1}$$

where the mean equivalent diameter, d_P, is given in Table 1. It should be noticed that Eq. (1) is valid for the following boundary conditions:

$$0.008 < \mathrm{Re} < 50$$

$$0.38 < d_P < 6 \text{ mm}$$

Both boundary conditions are fulfilled in this work.

The molecular diffusivity D_M, calculated using the Chapman–Enskog equation, and the axial dispersion coefficient, D_L, were calculated for the binary mixtures He/CO_2 and He/CH_4 within the temperature and pressure ranges covered by the experimental work. These values were also utilized in the ternary system. This approximation can be considered valid since the gas mixtures used in this work were very dilute. The numerical value of the axial dispersion coefficient $(D_L)_A$ for the binary mixture He/CO_2 was in the 25×10^{-6} to 29×10^{-6} m^2/s range within the temperature and pressure range of 40–60°C and 1.5–2.3 bar, respectively. The corresponding numerical value for the binary mixture He/CH_4, $(D_L)_B$, was in the 28×10^{-6} to 31×10^{-6} m^2/s range.

MATHEMATICAL MODELING AND NUMERICAL SIMULATION

To simulate the adsorption process in packed beds, an equilibrium model was used. The term "equilibrium model" refers to the assumption that instant local equilibrium is reached throughout the bed between the

bulk flow and the adsorbed phase (25). Equilibrium operation is not often found, but the condition is approached at low flow rates. At the same conditions, dispersion along the column could be significant. In this model the effects of all mechanisms which contribute to axial mixing are lumped together into a single effective axial dispersion coefficient. This is referred to as the "axial dispersed plug flow model" (26). This approach, which is particularly useful when the multicomponent equilibria can be represented in terms of an extended Langmuir relationship, has been frequently used (26–38).

The mathematical model was developed to handle systems where the adsorbable components were present only in small quantities, so-called trace systems. This means that the following approximations could be made:

The system was considered to be isothermal. Thermal effects due to heats of adsorption and desorption were neglected.
The superficial velocity through the column was assumed constant. Velocity effects due to adsorption were thus neglected.

In addition, it was assumed that:

The ideal gas law was applicable (the compressibility factors for the gas mixtures operated under the conditions used in the experiments were calculated to be greater than 0.99).
The frictional pressure drop in the bed was calculated to be negligible.
There was no radial concentration gradient.
Adsorption isotherms could be described by the Langmuir theory.

Based on these assumptions, the material balance equation for a multicomponent mixture can now be written

$$\left(\frac{\partial C_i}{\partial t}\right) + \frac{u}{\epsilon_v}\left(\frac{\partial C_i}{\partial L}\right) - D_L\left(\frac{\partial^2 C_i}{\partial L^2}\right) + \psi\left(\frac{\partial \bar{q}_i}{\partial t}\right) = 0 \tag{2}$$

where

$$\psi = \left(\frac{1 - \epsilon_v}{\epsilon_v}\right)\rho_s \tag{3}$$

together with the Danckwerts boundary conditions:

$$\left(\frac{\partial C_i}{\partial L}\right) = \frac{u}{D_L \epsilon_v}\left(C_i^F - C_i\right), \qquad L = 0,\ t > 0 \tag{4}$$

$$\left(\frac{\partial C_i}{\partial L}\right) = 0, \qquad L = L_0,\ t > 0 \tag{5}$$

and the initial conditions:

$$C_i(L, 0) = C_{i0}(L), \qquad t = 0, L > 0 \tag{6}$$

$$q_i(L, 0) = q_{i0}(L), \qquad t = 0, L > 0 \tag{7}$$

The equilibrium amount adsorbed is described by the Langmuir adsorption isotherm for a multicomponent system:

$$q_i^* = \frac{b_i q_{i\infty} C_i}{1 + \sum_{j=1}^{N} b_j C_j} \tag{8}$$

In the case of two adsorbable components together with one inert component, straightforward derivation yields for the first adsorbable component A:

$$\left(\frac{\partial C_A}{\partial t}\right) = \frac{1}{1 + \xi(1 + b_B C_B)}\left[-\frac{u}{\epsilon_v}\left(\frac{\partial C_A}{\partial L}\right) + (D_L)_A\left(\frac{\partial^2 C_A}{\partial L^2}\right) + \xi b_B C_A\left(\frac{\partial C_B}{\partial t}\right)\right] \tag{9}$$

where

$$\xi = \frac{\psi b_A q_{A\infty}}{(1 + b_A C_A + b_B C_B)^2} \tag{10}$$

A similar equation yields for the second adsorbable component B. The concentration C_B is set to zero in the case of just one adsorbing component.

These equations were solved numerically using a Crank–Nicolson finite difference discretization scheme which is unconditionally stable. The resulting nonlinear system of equations was solved iteratively using the Gauss–Seidel method.

RESULTS AND DISCUSSION

The experimental conditions are, except for the total pressure, given in each figure. The total pressure of the system was, if not otherwise mentioned, 2.3 bar.

Binary Mixture Experiments

A comprehensive number of experiments were conducted for both CO_2 and CH_4 (39) to study the influence of temperature, superficial velocity, and inlet partial pressure on the breakthrough behavior. The influence of

temperature and adsorbate concentration on the breakthrough behavior was examined for both species, while the influence of superficial velocity was studied for only carbon dioxide. The results obtained are displayed in Figs. 4–7.

Influence of Temperature

Figure 4 shows the breakthrough curves of CH_4 and CO_2 at 40 and 60°C. The curve profiles are almost symmetrical around the half-value point, $C_i/C_i^F = 0.5$. It can also be observed that the slope at the half-value point is steeper and the mean retention time much shorter at the higher temperature.

Influence of Superficial Velocity

Figure 5 shows that the breakthrough curve at the lower superficial velocity is much more dispersed than the curve at the higher velocity. It can also be seen that the residence time decreases with increasing velocity.

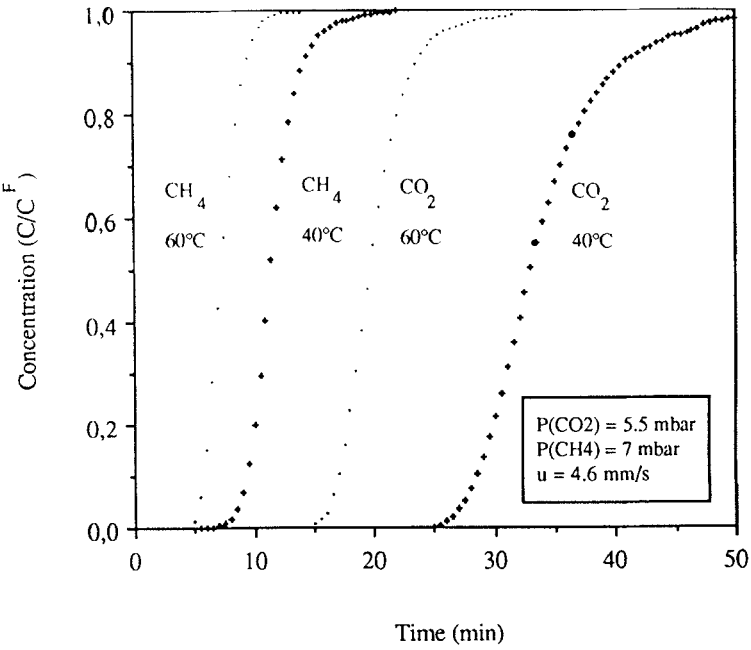

FIG. 4 Breakthrough curves of CH_4 and CO_2 at 40 and 60°C.

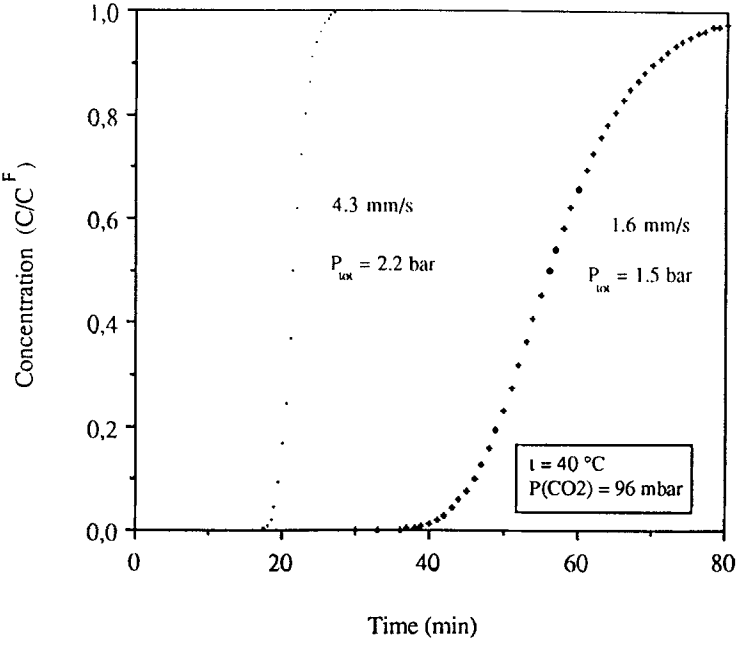

FIG. 5 Breakthrough curves of CO_2 at two different superficial velocities.

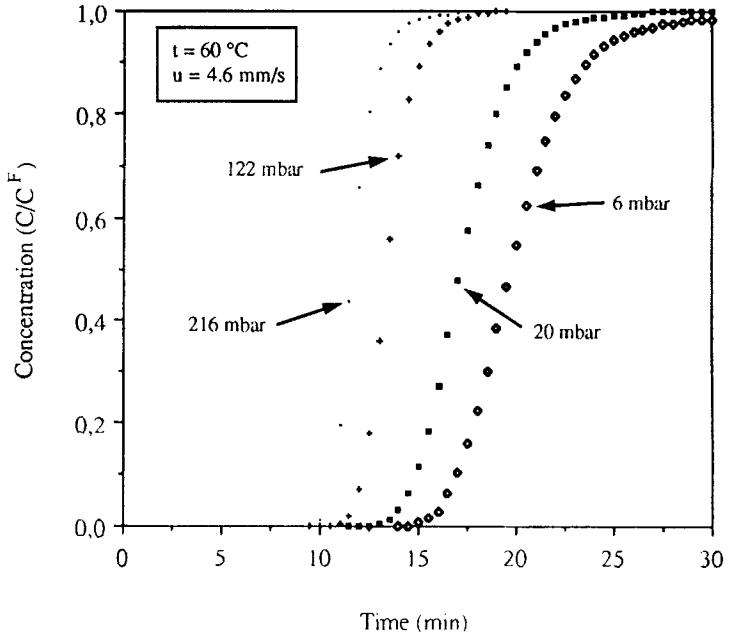

FIG. 6 Breakthrough curves of CO_2 at four different inlet partial pressures.

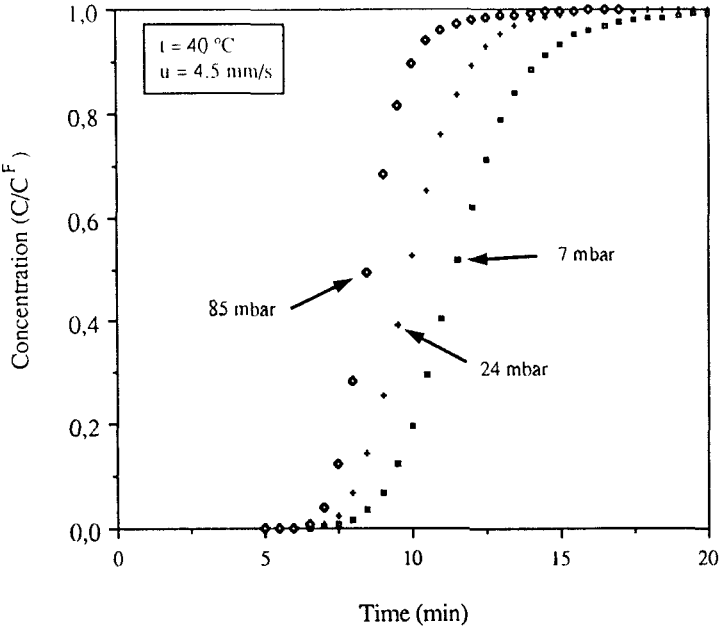

FIG. 7 Breakthrough curves of CH_4 at three different inlet partial pressures.

Other experiments clearly indicated that the influence of superficial velocity on the shape of the breakthrough curve could be neglected at velocities above 3.5 mm/s.

Influence of Inlet Partial Pressure

Figure 6 shows breakthrough curves for CO_2 at four different inlet partial pressures and 60°C, while the corresponding curves for CH_4 at 40°C are displayed in Fig. 7. As can be seen, the slope at the half-value point increases and the time elapsed before breakthrough decreases when the partial pressure in the feed increases. This behavior is more pronounced for CO_2 than for CH_4, and it is also more evident at the lower temperature.

This parametric study confirmed the expected breakthrough behavior a priori. Consequently, the breakthrough curves become more compressed with increasing temperature, concentration, and superficial velocity, and they become dispersed when these parameters decrease. Also, the fact that the operating parameters influenced the mean residence time was known a priori.

More importantly, the experimental work conducted in this study revealed the quantitative influence of the operating conditions on the pro-

cess behavior. Consequently, appropriate numerical intervals with a direct impact on the operating variables investigated were established for this process. The temperature interval from 40 to 60°C was large enough to exhibit remarkable changes in the breakthrough curves. The mean residence time was almost halved and the curves obviously steepened.

The influence of the superficial velocity on the shape of the breakthrough curve is more pronounced at the lower velocity of 1.6 mm/s and is negligible at 3.5 mm/s. The impact of the mean residence time, however, was never negligible. It should be noted that all other conditions could not be held constant when the study of the superficial velocity was studied due to restrictions of the experimental setup. The total pressure is therefore slightly different for the compared curves, but this difference is of minor importance compared to the large difference in the velocity.

The influence of concentration on the shape of the breakthrough curve is also large at partial pressures up to 100 mbar and less pronounced at higher partial pressures.

Adsorption Isotherms and Equilibrium Parameters

The results of the calculation of the adsorption isotherms for both CO_2 and CH_4, using the breakthrough curves from the binary mixture experiments, are given in Fig. 8. As can be observed, the shape of the adsorption isotherm is more favorable for CO_2 than for CH_4, and the adsorptive capacity of the bed is much higher for carbon dioxide at equal partial pressures. The isothermal data for each species were curve fitted to the Langmuir model; the calculated Langmuir equilibrium parameters can be found in Table 3. As can be seen, the Langmuir model could not describe the carbon dioxide isotherms in the whole concentration interval with a single set of parameters. Two sets of equilibrium parameters were therefore calculated for this component. On the other hand, the methane isotherms could be described well with only one set of Langmuir equilibrium parameters. This was expected because the concentration interval for methane was smaller and also because the methane isotherms are almost linear, as can be seen in Fig. 8.

It should be noticed that the model predictions for the ternary mixture experiments were performed using equilibrium parameters determined from the binary mixture experiments. The parameters used in these simulations can therefore be considered to be independently determined.

Ternary Mixture Experiments

The main objective of conducting these experiments was to study the influence of the competitive adsorption of CH_4 and CO_2 on the breakthrough behavior of the adsorbates, and to determine the extent of separa-

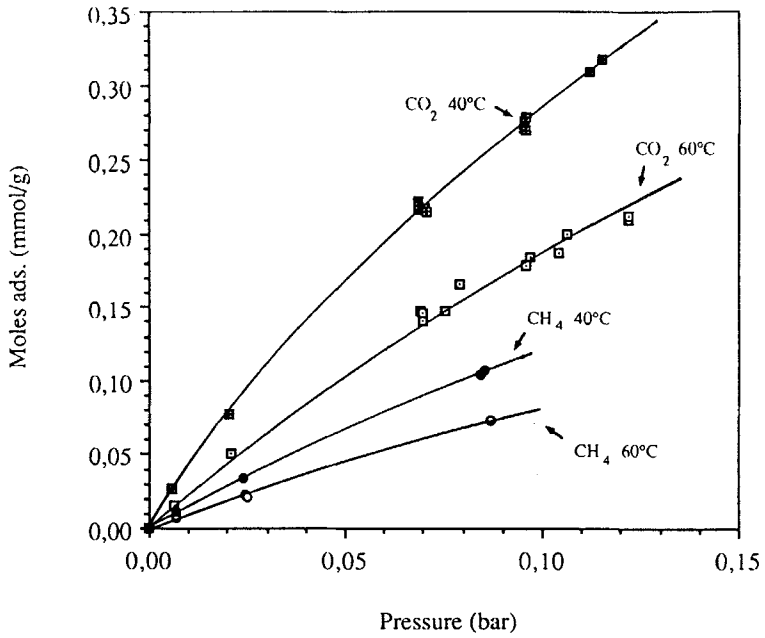

FIG. 8 Adsorption isotherms for CO_2 and CH_4 at 40 and 60°C.

TABLE 3
Calculated Values of the Separation Factor ($\alpha_{CO_2-CH_4}$)

Temperature (°C)	Inlet partial pressure (mbar)		Separation factor (—)
	CO_2	CH_4	
40	7	6	2.9
40	24	23	3.3
40	84	81	3.5
60	7	7	2.7
60	25	24	2.7
60	85	81	2.8
40	Independent of composition		2.2
60	Independent of composition		3.5

tion of these two adsorbates. The experimental breakthrough curves had similar responses to changes in temperature and inlet partial pressure as those obtained from binary mixture experiments. The results clearly showed that the methane concentration exceeded the feed concentration at a certain time interval. This rollover behavior is negligible at the lowest concentration and became more pronounced at higher concentrations.

The experimental data revealed the competitive nature of the two adsorbate systems. Since CO_2 is more strongly held by the adsorbent, it tends to displace the previously adsorbed CH_4 and causes the methane breakthrough curve to exceed the influent concentration level, i.e., to rollover. The characteristics of this behavior were previously predicted (11) using a semiempirical rate model for adsorption under constant pattern conditions. The relationship between the concentration distributions of CO_2 and CH_4 may be seen more clearly in Fig. 9 where the predicted gas-phase compositions are plotted as a function of the bed length at two different times. As can be seen, after the elapse of 4 minutes the desorbed methane is carried forward by the gas flow and its gas-phase concentration is increased above the inlet value both in and downstream of the carbon

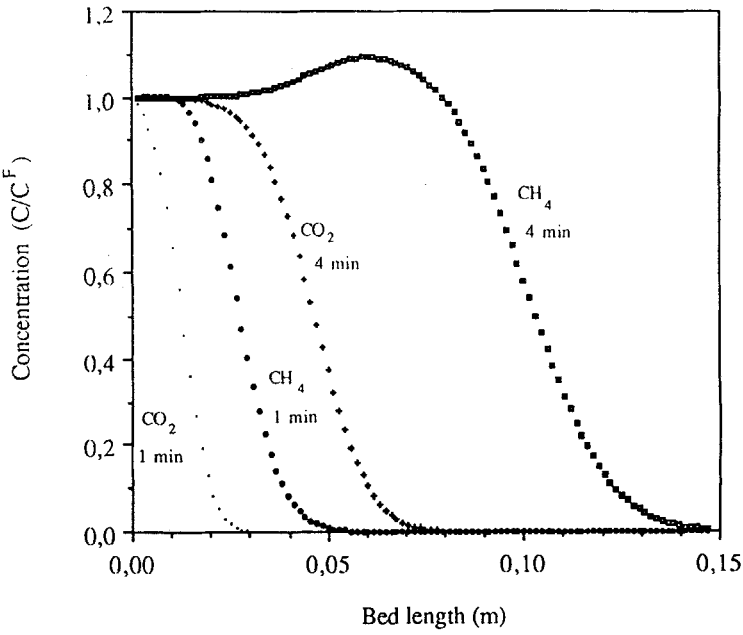

FIG. 9 Calculated CO_2 and CH_4 gas-phase concentrations in the adsorbent bed at various times.

dioxide zone. Consequently, four zones are generated during the adsorption in the carbon bed where both adsorbates are present in the upper zones while only the weak adsorbate, CH_4, is present in the lower zones. It should be mentioned that the influence of competitive adsorption on breakthrough behavior was negligible at partial pressures smaller than 7 mbar. This can be attributed to the fact that the adsorption capacity of the adsorbent bed is high enough at low adsorbate concentrations to embrace both species without any competition.

To quantify the extent of competitive adsorption of CO_2 and CH_4, the separation factor for the activated carbon was calculated using both experimental breakthrough curves and equilibrium ratios obtained by the Langmuir isotherm constants. The results are summarized in Table 4. Both species are better separated at the lower temperature and higher inlet partial pressures. The separation factors calculated using experimental data are 3.0–3.5 at 40°C and 2.7–2.8 at 60°C. The activated carbon used in this study should therefore be an interesting adsorbent candidate for the separation of CO_2 and CH_4 mixtures. As can be observed from Table 4, the separation factors calculated using equilibrium ratios are in contradiction compared to those calculated using experimental data. This indicates that the Langmuir model is not appropriate to describe the adsorption behavior of this multicomponent system.

Comparison with Binary Mixture Experiments

As stated earlier, the mathematical model was formulated in this study to simulate adsorption systems for transient adsorption of diluted gas mixtures. Figure 10 shows the results from model calculations compared to experimental breakthrough curves for methane at 60°C and two different inlet partial pressures. An analysis of the effect of the single component parameters on the breakthrough curve revealed that the dispersion coeffi-

TABLE 4
Langmuir Equilibrium Parameters

Temperature (°C)	Partial pressure (mbar)	Carbon dioxide		Methane	
		b_i (m^3/mol)	$q_{i\infty}$ (mmol/g)	b_i (m^3/mol)	$q_{i\infty}$ (mmol/g)
40	<85	0.202	0.607	0.092	0.457
40	85–220	0.068	1.390	—	—
60	<85	0.164	0.473	0.047	0.529
60	85–220	0.070	0.940	—	—

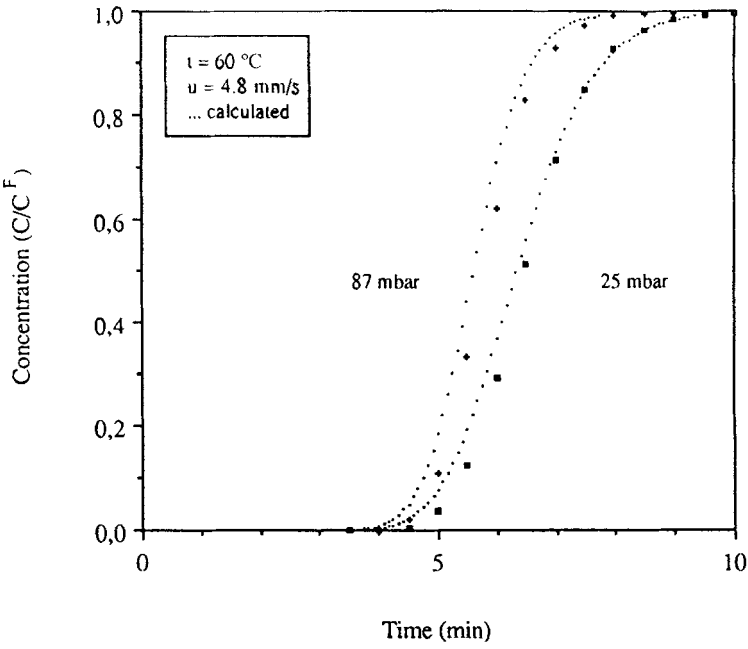

FIG. 10 Calculated and experimental breakthrough curves of CH_4 at 60°C and two different inlet partial pressures.

cient does not play a significant role in the shape of the curve. The most important parameters were those related to the adsorption isotherm.

Comparison with Ternary Mixture Experiments

Figures 11–13 demonstrate the results of model simulations of breakthrough curves compared to experimental data of the ternary system at 40 and 60°C for a lower and higher inlet partial pressure of the adsorbates. As can be seen, the agreement between model simulations and experimental data can be considered satisfactory. There is, however, a considerable deviation between the calculated and experimental curves at the higher inlet partial pressure at 40°C. Compared to experimental data, the model simulations yield a shorter mean residence time for the CO_2 front and a smaller rollover for the CH_4 front. The deviation may be attributed to the failure of the Langmuir model to correctly calculate the actual capacity of the bed. This may also be the reason behind the contradictory results obtained when the separation factors for the activated carbon were calculated using both experimental data and equilibrium ratios.

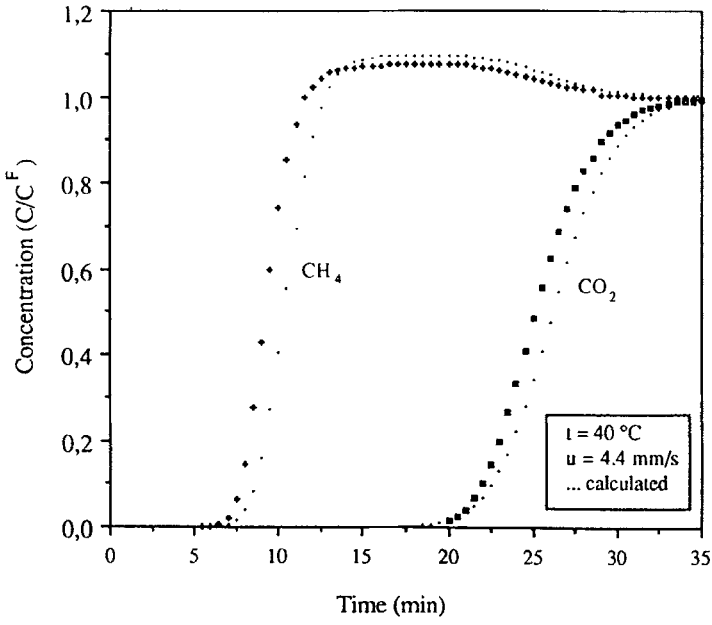

FIG. 11 Calculated and experimental breakthrough curves for the binary adsorption of CO_2 and CH_4 at 40°C with $P_{CO_2} = 24$ and $P_{CH_4} = 23$ mbar.

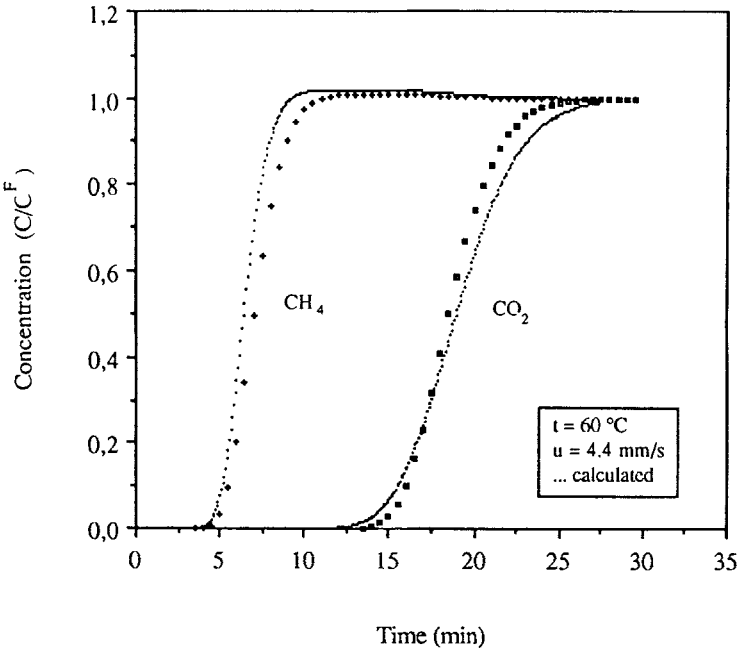

FIG. 12 Calculated and experimental breakthrough curves for the binary adsorption of CO_2 and CH_4 at 60°C with $P_{CO_2} = P_{CH_4} = 7$ mbar.

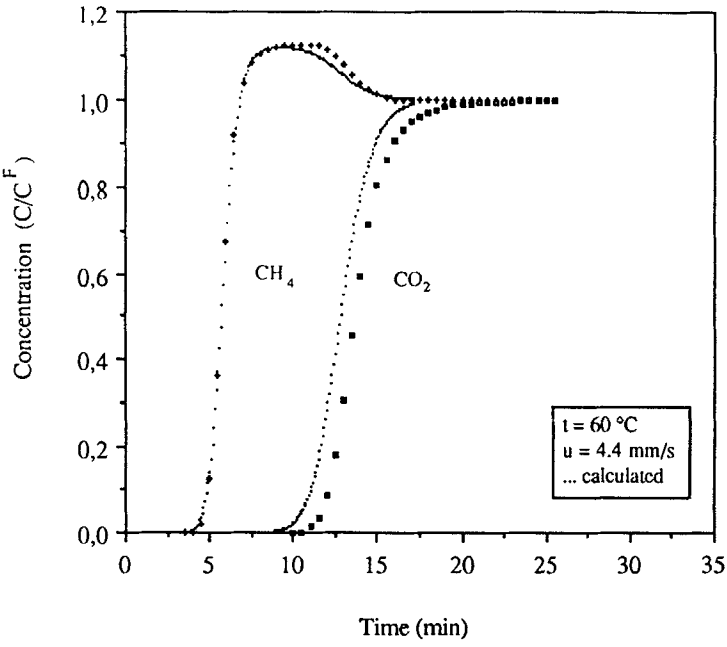

FIG. 13 Calculated and experimental breakthrough curves for the binary adsorption of CO_2 and CH_4 at 60°C with P_{CO_2} = 85 and P_{CH_4} = 81 mbar.

The Desorption Process

The calculation of breakthrough curves for the desorption process of both binary and ternary mixture systems can be achieved by the same mathematical model. Figure 14 shows calculated and experimental breakthrough curves for the desorption process of CO_2 and CH_4 at both 40 and 60°C. As can be seen, the desorption breakthrough curves for CO_2 are more dispersed than the corresponding adsorption curves. The same is not valid for CH_4 since the desorption curves for this component are almost mirror reflections of the corresponding adsorption curves. This behavior can be attributed to the fact that the adsorption isotherms are favorable for CO_2 and almost linear for CH_4.

The agreement between the calculated and experimental breakthrough curves for the single component case is very good, with the exception for CH_4 at 40°C where the model tends to overpredict the concentration front which results in a longer mean residence time.

A typical desorption breakthrough curve for the ternary mixture (CO_2/CH_4/He) experiments is shown in Fig. 15. The agreement between the calculated and experimental breakthrough curve is better for CH_4 than

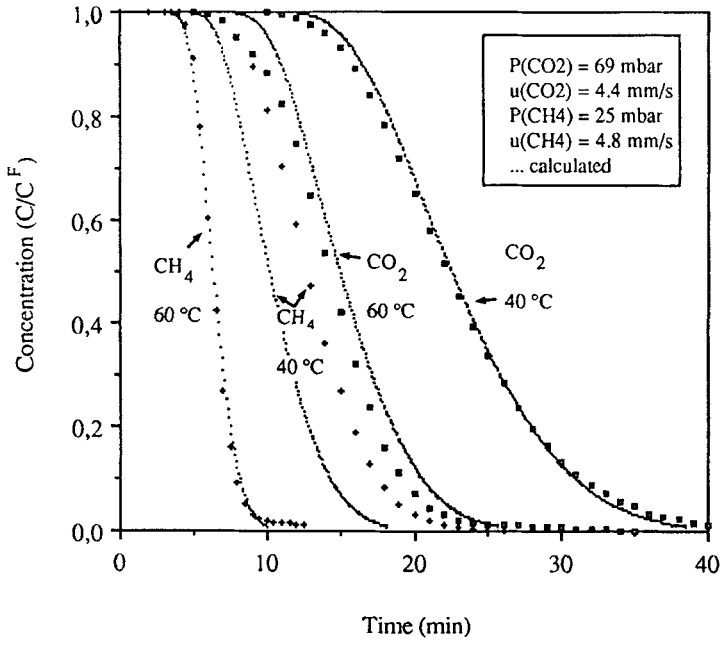

FIG. 14 Calculated and experimental desorption breakthrough curves for CO_2 and CH_4 at 40 and 60°C.

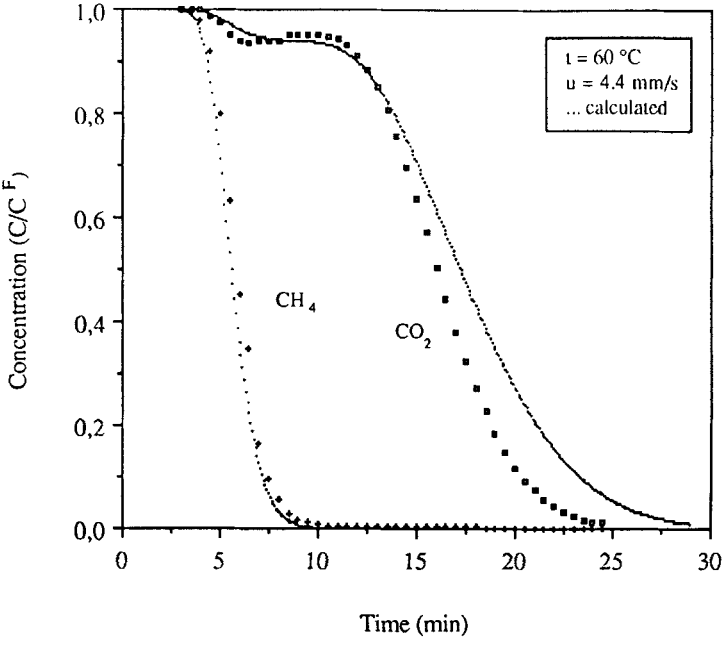

FIG. 15 Calculated and experimental desorption breakthrough curves for the CO_2/CH_4/He mixture at 60°C with P_{CO_2} = 25 and P_{CH_4} = 24 mbar.

for CO_2. As can be seen, the desorption curve for CO_2 can be divided into three zones. An initial decrease in concentration comes earlier than the corresponding behavior of the single component curve. This zone is followed by a plateau of constant concentration. The experimental curve in this zone is divided into two distinct steps where the concentration is overshooting in the lower part of the curve. This behavior is physically unrealistic and is attributed to the fact that the CO_2 concentration was calculated as the difference between the TCD and the FID signals. This may give a slightly larger error when the effluent concentration of CH_4 is changing rapidly. In the third zone, the calculated and experimental CO_2-desorption curves diverge. Whereas the form of adsorption curves is dictated mainly by dispersion, the desorption curves are sensitive to the form of the adsorption isotherm. A simple Langmuir adsorption equation is appropriate for methane, and the experimental and calculated CH_4-desorption curves agree fairly well. The adsorption of CO_2, on the other hand, cannot be described using the simple Langmuir equation at lower CO_2 concentrations, as is shown in Table 3 where two straight regions are distinguished. As the real curve will be smooth, an underestimate in the amount adsorbed results in lower CO_2 concentrations which, in turn, will result in an overestimation of the calculated residence times.

CONCLUSIONS

A parametric study was conducted to establish the influence of temperature, superficial velocity, and inlet partial pressure on the breakthrough behavior of the adsorbates. The breakthrough curves showed a compressive behavior with increasing temperature, superficial velocity, and initial partial pressure. This behavior becomes less pronounced at superficial velocities greater than 3.5 mm/s and at initial partial pressure exceeding 100 mbar. The same trend is, however, not valid for the mean residence time. The ternary mixture experiments revealed the competitive nature of the two component adsorption. Since CO_2 is more strongly adsorbed, it tends to displace the previously adsorbed CH_4. This causes the breakthrough curve to rollover above its influent concentration level. However, this behavior disappears at low inlet partial pressures since the adsorptive capacity of the bed is high enough for coadsorption. The separation factor for the activated carbon used in this study was calculated to be 3.0–3.5 at 40°C and 2.7–2.8 at 60°C.

The mathematical model was designed to describe the adsorption and desorption processes for dilute gas mixtures containing two adsorbates. The model was based on approximations of local equilibrium, described by the extended Langmuir relationship, and isothermal conditions. The system of differential equations was solved numerically by a finite differ-

ence discretization scheme using the implicit method of Crank–Nicolson. The resulting nonlinear system of equations was solved iteratively using the Gauss–Seidel method. The different physicochemical parameters involved in the model were evaluated using both empirical correlations and experimental data. The model simulations for both the adsorption and desorption processes were generally in good agreement with experimental data for both the binary and ternary gas mixtures. There are, however, a few cases with considerable deviations which can be attributed to deficiencies in the Langmuir model itself. The extended Langmuir relationship should therefore be replaced by another equilibrium equation capable of a more accurate description of the adsorption isotherms in the entire concentration interval. The Langmuir–Freundlich equation may be more appropriate to use for this type of gas adsorption system.

By extending the mathematical model suggested in this work to cover a larger concentration interval, it could be a useful tool for the proper design of a CO_2 and CH_4 separation column applied in landfill gas purification processes. The procedure to determine the equilibrium data to be utilized in the mathematical model has a considerable potential in calculating column performance, and it can also reduce the number of experiments needed for the design of these columns.

SYMBOLS

b	Langmuir equilibrium constant (m^3/mol)
C	fluid phase concentration of adsorbate (mol/m^3)
C_0	fluid phase concentration of adsorbate at $t = 0$ (mol/m^3)
D_L	axial dispersion coefficient (m^2/s)
D_M	molecular diffusivity (m^2/s)
d_P	mean equivalent diameter of particles (m)
L	axial length coordinate (m)
L_0	adsorbent bed length (m)
N	number of components (—)
P_{CH_4}, P_{CO_2}	partial pressure of methane and carbon dioxide (mbar)
q	concentration in solid phase (mol/g)
q_0	concentration in solid phase at $t = 0$ (mol/g)
q_∞	loading capacity of adsorbent (mol/g)
Re	Reynolds number (—)
t	time (s)
u	superficial fluid velocity (m/s)

Greek

α	separation factor (—)
ϵ_v	voidage of adsorbent bed (—)

ξ	quantity defined by Eq. (10)
ψ	quantity defined by Eq. (3) (kg/m^3)
ρ_s	density of the adsorbent (kg/m^3)

Subscripts

A, B	adsorbate component A and B
i, j	adsorbate component i and j

Superscripts

F	feed stream
–	average value
*	equilibrium value

REFERENCES

1. D. M. Ruthven and C. B. Ching, *Chem. Eng. Sci.*, *44*, 1011 (1989).
2. P. C. Wankat, *Large Scale Adsorption and Chromatography*, CRC Press, Boca Raton, Florida, 1986.
3. R. T. Yang and A. Kapoor, *Chem. Eng. Sci.*, *44*, 1723–1733 (1989).
4. R. T. Pilarczyk and H. J. Schröter, in *Gas Separation Technology* (E. F. Vansant and R. Dewolfs, Eds.), Elsevier, 1989, pp. 271–279.
5. S. N. Vyas, S. R. Patwardhan, I. Gupta, and V. Burra, *Sep. Sci. Technol.*, *26*(10&11), 1419–1431 (1991).
6. N. Haq and D. M. Ruthven, *J. Colloid Interface Sci.*, *112*, 154 (1986).
7. J. W. Carter and H. Husain, *Chem. Eng. Sci.*, *29*, 267–273 (1974).
8. R. L. Gariepy and I. Zwiebel, *AIChE Symp. Ser.*, *67*(117), 17 (1971).
9. J. S. C. Hsieh, R. M. Turian, and C. Tien, *AIChE J.*, *23*, 263 (1977).
10. D. O. Cooney and E. N. Lightfoot, *Ind. Eng. Chem., Process Des. Dev.*, *5*, 25 (1966).
11. W. J. Thomas and J. L. Lombardi, *Trans. Inst. Chem. Eng.*, *49*, 240 (1971).
12. D. O. Cooney and F. P. Strusi, *Ind. Eng. Chem., Fundam.*, *11*, 123 (1972).
13. Y. Takeuchi, T. Wasai, and S. Suginaka, *J. Chem. Eng. Jpn.*, *11*, 458 (1978).
14. S. Sircar and R. Kumar, *Sep. Sci. Technol.*, *21*(9), 919–939 (1986).
15. E. Richter, *Erdöl Kohle*, *40*(9), 394–399 (1987).
16. Y. W. Wong and J. L. Niedzwiecki, *AIChE Symp. Ser.*, *78*, 120–127 (1982).
17. P. Jacob and D. Tondeur, *Chem. Eng. J.*, *22*, 187–202 (1981).
18. P. Jacob and D. Tondeur, *Ibid.*, *26*, 41–58 (1983).
19. K. Chihara and M. Suzuki, *J. Chem. Eng. Jpn.*, *16*(1), 53–61 (1983).
20. R. T. Yang, S. J. Doong, and P. L. Chen, *AIChE Symp. Ser.*, *81*, 84–94 (1985).
21. P. L. Chen, W. N. Chen, and R. T. Yang, *Ind. Eng. Chem., Process Des. Dev.*, *24*, 1201–1208 (1985).
22. P. L. Chen and R. T. Yang, *Ind. Eng. Chem., Fundam.*, *25*, 758–767 (1986).
23. Z. Z. Mutasim and J. H. Bowen, *Trans. IChemE*, *70*(A), 346–353 (1992).
24. M. F. Edwards and J. F. Richardson, *Chem. Eng. Sci.*, *23*, 109–123 (1968).
25. P. C. Wankat, *Rate-Controlled Separations*, Elsevier Applied Science, 1990, pp. 143–146.
26. D. M. Ruthven, *Principles of Adsorption and Adsorption Processes*, Wiley, New York, 1984, pp. 208–213.

27. K. Hashimoto, S. Adachi, H. Noujima, and A. Maruyama, *J. Chem. Eng. Jpn.*, *16*, 400–406 (1983).
28. M. Morbidelli, G. Storti, S. Carra, G. Niederjaufner, and A. Pontoglio, *Chem. Eng. Sci.*, *39*, 383–393 (1984).
29. M. Morbidelli, G. Storti, S. Carra, G. Niederjaufner, and A. Pontoglio, *Ibid.*, *40*, 1155–1167 (1985).
30. M. Morbidelli, G. Storti, R. Paludetto, and S. Carra, *Fundamentals of Adsorption* (A. I. Liapis, Ed.), Engineering Foundation, New York, 1987.
31. E. Santacesaria, M. Morbidelli, A. Servida, G. Storti, and S. Carra, *Ind. Eng. Chem., Process Des. Dev.*, *24*, 83–88 (1985).
32. G. Storti, E. Santacesaria, M. Morbidelli, and S. Carra, *Ibid.*, *24*, 89–92 (1985).
33. C. B. Ching and D. M. Ruthven, *Can. J. Chem. Eng.*, *62*, 398–403 (1984).
34. C. B. Ching and D. M. Ruthven, *AIChE Symp. Ser.*, *81*(242), 1–8 (1985).
35. C. B. Ching and D. M. Ruthven, *Chem. Eng. Sci.*, *40*, 877–885 (1985).
36. C. B. Ching, D. M. Ruthven, and K. Hidjat, *Ibid.*, *40*, 1411–1417 (1985).
37. C. B. Ching, D. M. Ruthven, and K. Hidjat, *Ibid.*, *41*, 2953–2956 (1986).
38. G. Carta and R. L. Pigford, *Ind. Eng. Chem., Fundam.*, *25*, 677–685 (1986).
39. M. Andersson, "Separation of CO_2 and CH_4 by Adsorption on Activated Carbon," M.Sc. Thesis, Lund University, Sweden, LUTKDH/(TKKA-5025)/1-93/(1991).

Received by editor April 17, 1992
Revised April 20, 1993